Searches for Extra Dimensions and for Heavy Resonances in Dilepton, Diphoton, Electron + Photon and Electron + Missing $\mathrm{E_T}$ Final States with the DØ Detector

Carsten Magass on behalf of the DØ Collaboration [a]

III. Physikalisches Institut A, RWTH Aachen, D-52056 Aachen (Germany)

Abstract. The high mass spectrum of lepton and photon pairs is sensitive to a broad array of new physics. Examples include searches for extra dimensions in the dielectron and diphoton channels. A direct search for electron compositeness is possible in the production of excited electrons decaying into an electron and a photon. In addition, the electron plus missing transverse energy data sample can be searched for a W' boson. Latest results in searches in the high mass dielectron, diphoton, electron plus photon, and electron plus missing transverse energy channels obtained by the DØ experiment at the Tevatron are reported, using a data set corresponding to an integrated luminosity of about 1 fb^{-1}. Since no significant excess is observed in the data in all cases, limits are set which improve on previous searches.

PACS. 12.60.-i Models beyond the standard model – 13.85.Rm Limits on production of particles

1 Introduction

The standard model (SM) describes the fundamental fermions and their interactions via gauge bosons at a high level of accuracy, but it is not considered to be a complete theory. Some aspects – like the number of fermion families and the hierarchy problem – remain unexplained. Many possible extensions to the SM have been proposed, which usually predict new particles and contain new parameters. These new particles and their decays can be looked for at a collider experiment like the proton-antiproton collider Tevatron which currently (Run II) operates at a center-of-mass energy of $\sqrt{s} = 1.96$ TeV, thus being the world's most energetic particle collider until the startup of the Large Hadron Collider (LHC). At these colliders, it is possible to produce particles with extremely high masses that could never be explored before.

The Tevatron collider is performing very well; an integrated luminosity of more than 3 fb^{-1} has already been delivered. Three recent analyses [1] are presented which use data taken with the DØ detector [2] until February 2006 (Run IIa). This dataset corresponds to a recorded luminosity of about 1 fb^{-1}. The data are searched for new particles introduced in different extensions to the SM via their decays into high energetic electrons, photons and neutrinos, where the latter ones give rise to missing transverse energy ($\not\!\!E_T$). The analyses make use of the capabilities to detect and identify such particles with the well understood DØ detector.

[a] *Email:* magass@fnal.gov

2 Randall-Sundrum Extra Dimensions

The hierarchy problem posed by the large difference between the Planck scale $M_{\mathrm{Planck}} \approx 10^{16}$ TeV, at which gravity is expected to become strong, and the scale of the electroweak symmetry breaking at ≈ 1 TeV can be solved by the introduction of extra spatial dimensions. In the model of Randall and Sundrum [3] the gravity originating on a (3+1)-dimensional brane (Planck brane) is separated from the SM brane in a 5^{th} dimension with a warped metric. Gravity appears weak at the SM brane due to the exponential suppression caused by the metric. In the simplest version of this model the only particles that can propagate in the extra dimension are gravitons, which appear as towers of Kaluza-Klein excitations with masses and widths that are determined by the parameters of the model: the mass of the first excited mode of the graviton, M_1, and a dimensionless coupling to SM fields, $k\sqrt{8\pi}/M_{\mathrm{Planck}}$. Precision electroweak data and the requirement that the model remains perturbative constrain the coupling to lie between about 0.01 and 0.1.

The resonant production of the first excited graviton mode and its decay into dielectron and diphoton pairs are investigated, $p\bar{p} \rightarrow G + X \rightarrow ee/\gamma\gamma + X$. The dielectron pairs from the decaying graviton with spin 2 are in a p-wave state, whereas the $\gamma\gamma$ pairs can also be in an s-wave state. Because of this the branching fraction into $\gamma\gamma$ is twice the branching fraction into ee.

Data events are selected if they are triggered and contain two isolated objects in the central electromagnetic (EM) calorimeter ($|\eta| < 1.1$) with transverse energy $E_T > 25$ GeV. Further, the energy deposition pat-

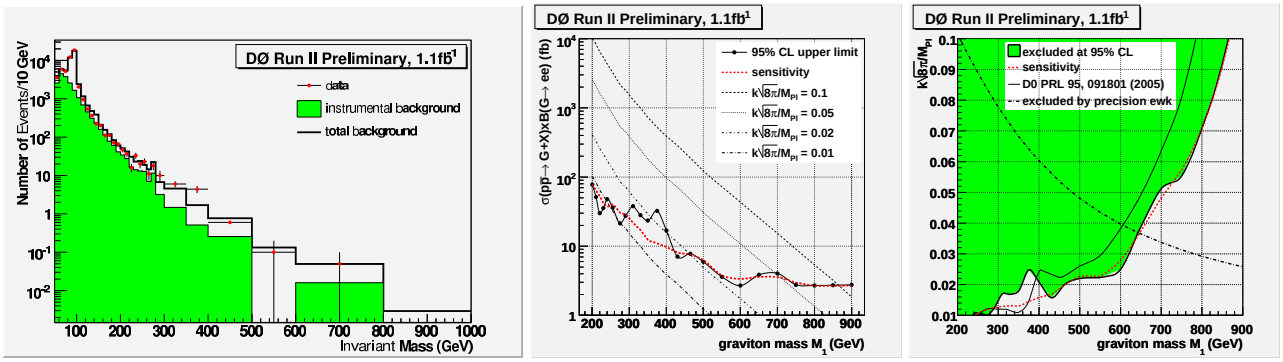

Fig. 1. Left: invariant mass spectrum of the two EM objects; middle: 95% CL upper limit on the production cross section times branching fraction compared with the sensitivity and theoretical prediction for various values of the coupling; right: 95% CL exclusion contour in the $(k\sqrt{8\pi}/M_{\rm Planck}, M_1)$-plane compared with the sensitivity and the previously published contour.

terns of the two objects are required to be consistent with EM showers. A track match criterion is omitted in order to accept both $\gamma\gamma$ and ee decay channels. The dataset contains 50,354 events with an invariant mass of the two EM objects above 50 GeV.

Physics backgrounds (Drell-Yan production of ee and direct $\gamma\gamma$ production) are simulated using PYTHIA [4] Monte Carlo samples. Differences in reconstruction efficiencies observed in data and Monte Carlo are taken into account. Instrumental backgrounds, in which one or both of the EM objects are misidentified, are estimated from data. For this purpose a dataset is used which contains two EM objects that fail the tight EM shower criteria. This provides an estimate for the shape of the invariant mass spectrum of the instrumental background. In order to determine the relative contribution of this background, the invariant mass spectrum is fitted around the Z peak (60 GeV $< m_{ee} <$ 140 GeV) with the sum of physics and instrumental backgrounds, see Fig. 1 (left).

The spectrum above 140 GeV is searched for a possible graviton signal. This is accomplished by constructing a sliding mass window, which is optimized with respect to the sensitivity for a given graviton mass. Systematic uncertainties on the signal and background samples are of the order of 10%.

Since no significant deviation from the background prediction is observed, upper limits on the production cross section times branching fraction, $\sigma(p\bar{p} \rightarrow G + X) \times B(G \rightarrow ee)$, are calculated using a Bayesian approach [5] with a flat prior. The resulting 95% confidence level (CL) limits (expected and observed) as a function of the graviton mass are shown in Fig. 1 (middle) and compared to the theoretical predictions for various values of the coupling parameter. Fig. 1 (right) displays the 95% CL exclusion contour in the $(k\sqrt{8\pi}/M_{\rm Planck}, M_1)$-plane. Hence, masses for the first excited graviton mode below 865 GeV (240 GeV) can be excluded at the 95% CL for $k\sqrt{8\pi}/M_{\rm Planck} = 0.1$ (0.01).

3 Excited Electrons

In several models the observation of three families of fundamental fermions is explained by postulating that quarks and leptons are composed of scalar and spin-1/2 particles. In compositeness models [6] the underlying substructure leads to a large spectrum of excited states. In this analysis the production of excited electrons e^* via contact interaction (CI) and the subsequent electroweak decay $e^* \rightarrow e\gamma$ is investigated, $p\bar{p} \rightarrow ee^* + X \rightarrow ee\gamma + X$. The (gauge mediated) electroweak production of excited electrons is neglected due to its smallness compared to production via CI. Possible contributions from CI decays are taken into account in the decay width. Free parameters in this model are the compositeness scale Λ and the mass of the excited electron m_{e^*}.

Data events are selected if they are triggered and contain two isolated electrons within $|\eta| < 1.1$ (CC) or $1.5 < |\eta| < 2.5$ (EC) with transverse energies $E_T >$ 25 GeV for the leading electron and $E_T > 15$ GeV for the second leading electron. The electrons are required to have energy deposition patterns consistent with EM showers, to be spatially separated, and to have an associated track. Combinations with both electrons found in opposite EC's are rejected.

This dataset is compared to the background prediction, consisting of PYTHIA [4] Monte Carlo samples for the physics backgrounds ($Z/\gamma^* \rightarrow ee$, $Z/\gamma^* \rightarrow \tau\tau \rightarrow eeX$ etc.) and a special sample for the instrumental background. The latter one is due to QCD multijet events with jets misidentified as electrons, and can be (similar to the Randall-Sundrum analysis) estimated from data. The normalization of the multijet sample is adjusted in the invariant mass interval 30 GeV $< m_{ee} <$ 65 GeV. The full dielectron data sample contains 62,930 events, which is compatible with the background expectation of 61,560 ± 6,553 events, see Fig. 2 (left).

Finally, an additional photon within the CC or EC region of the calorimeter with $E_T > 15$ GeV is selected. It is required to be separated from the two electrons, not to have a track associated, to be isolated and to fulfill tight EM shower constraints. The $ee\gamma$

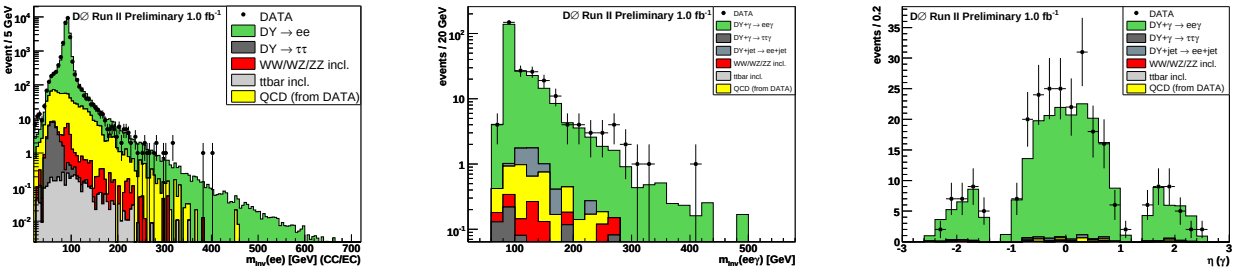

Fig. 2. Left: invariant mass distribution of the two electrons m_{ee} (CC/EC combination); middle: invariant mass distribution of the two electrons and the photon $m_{ee\gamma}$; right: η distribution of the photon.

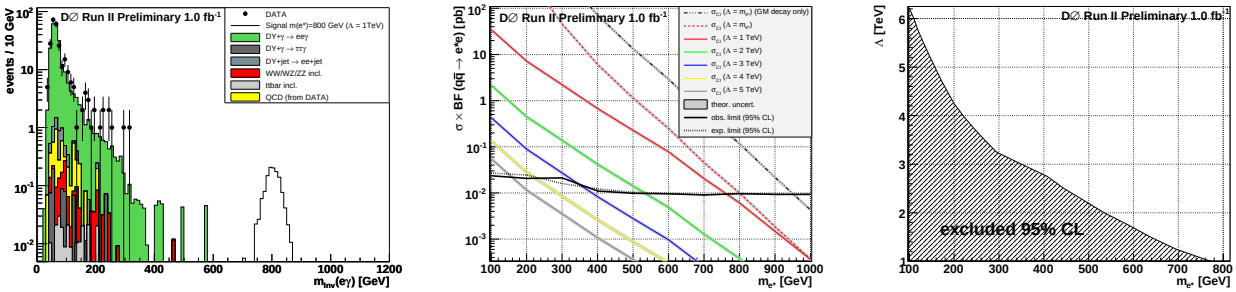

Fig. 3. Left: invariant mass distribution of the electron and photon (combination closest to $m_{e^*} = 800$ GeV); middle: 95% CL upper limits on the production cross section times branching fraction as a function of the e^* mass m_{e^*}; right: 95% exclusion contour as a function of the compositeness scale Λ and the excited electron mass m_{e^*}.

dataset contains 259 events, while 232 ± 29 events are expected from background processes, see Fig. 2 (middle and right). Systematic uncertainties (backgrounds 10%, signal 15%) come from efficiency corrections, the luminosity, estimation of the photon misidentification rate, multijet estimation, cross sections and PDF uncertainties.

A crucial point is the reconstruction of the $e\gamma$ invariant mass, where the excited electron would be observable as a resonance. Depending on the mass of the excited electron two different approaches are considered: For $m_{e^*} \leq 200$ GeV the lower energetic electron and the photon are combined; otherwise the combination closest to the searched e^* mass is chosen. Fig. 3 (left) shows the $e\gamma$ invariant mass distribution for an excited electron with $m_{e^*} = 800$ GeV. In order to further enhance the sensitivity for light excited electrons, combinations where both electrons and the photon are reconstructed in the EC are rejected (for $m_{e^*} \leq 300$ GeV), and a tighter cut on the spatial separation between the photon and the electron with lower energy is applied (for $m_{e^*} \leq 200$ GeV).

Since no significant excess is observed in the data, upper limits are set on the CI production cross section times branching fraction, $\sigma(p\bar{p} \to ee^* + X) \times B(e^* \to e\gamma)$, using a Bayesian approach [5]. A final cut is applied in the $e\gamma$ invariant mass distribution, which is optimized with respect to the expected limit. The 95% CL limits on the cross section as a function of the excited electron mass m_{e^*} are shown in Fig. 3 (middle), and compared to the theoretical prediction for various values of the compositeness scale Λ. The 95% exclusion contour as a function of Λ and m_{e^*} is displayed in Fig. 3 (right). The lower mass limit for $\Lambda = 1$ TeV is $m_{e^*} > 756$ GeV, for $\Lambda = m_{e^*}$ the resulting lower mass bound is 796 GeV. If CI decays are neglected, a mass limit of $m_{e^*} > 946$ GeV is derived for $\Lambda = m_{e^*}$, thus improving the previous mass limit of $m_{e^*} > 879$ GeV set by the CDF collaboration [7].

4 New Heavy Charged Gauge Bosons

Additional charged gauge bosons W' (as well as additional neutral gauge bosons Z') are introduced in many extensions to the SM, e. g. Left-Right-Symmetric models (broken $\mathrm{SU}(2)_L \otimes \mathrm{SU}(2)_R$) or in GUT models which may also imply supersymmetry (e. g. E_6), see [8]. In some models the W' boson is right-handed, and decays therefore into a right-handed neutrino and a charged lepton. However, such a neutrino has not yet been observed. Assuming the most general case, the new gauge group can comprise a new mixing angle ξ, new couplings to the fermions g' and a new CKM matrix U'. We make the assumptions that there is no mixing, g' is equal to the SM coupling, U' is equal to the SM CKM matrix, and that the new decay channel $W' \to WZ$ is suppressed [9]. Furthermore, the width $\Gamma_{W'}$ of the W' boson is assumed to scale with its mass $m_{W'}$. The decay into the third quark family (e. g. $W' \to t\bar{b}$), which is possible for $m_{W'}$ above 180 GeV, is taken into account. In case of the existence of additional generations of fermions, it is assumed that they are too heavy to be produced by a W' decay. In this analysis the decay $W' \to e\nu$ is investigated.

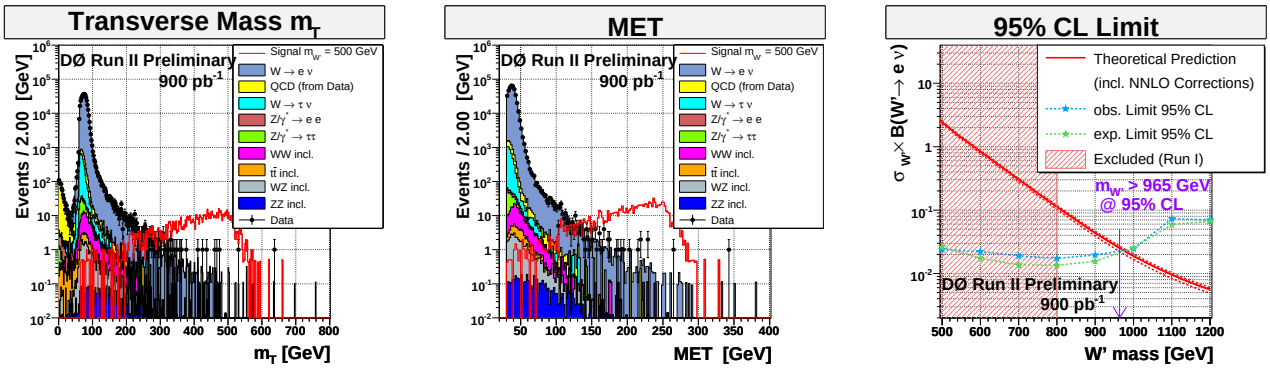

Fig. 4. Left: transverse mass m_T distribution; middle: missing transverse energy $\not\!\!E_T$ distribution; right: 95% CL upper limit on the production cross section times branching fraction as a function of the W' boson mass $m_{W'}$.

Data events are selected if they are triggered, exhibit missing transverse energy $\not\!\!E_T > 30$ GeV and contain an electron with transverse energy $E_T > 30$ GeV within $|\eta| < 1.1$. The electron is required to be isolated in the calorimeter and to have a track matched in z and ϕ direction. The energy deposition pattern of the electron is required to be consistent with EM showers. Further cleaning cuts (e. g. no jet activity in opposite direction of the electron or $\not\!\!E_T$) are applied in order to reject misidentified $\not\!\!E_T$ and the multijet background.

Several SM processes lead to the electron + $\not\!\!E_T$ final state, like $W \to e\nu$ or $W \to \tau\nu \to e\nu X$. These backgrounds are estimated using PYTHIA [4] Monte Carlo samples. Events from multijet production can also contribute if one jet is misidentified as an electron and large $\not\!\!E_T$ is caused by energy mismeasurement. This contribution is estimated from a special data sample. In this sample the electron candidate fails the tight shower shape requirement. The resulting events are scaled to the data sample. The scale factor is adjusted in the low reconstructed mass region ($m_T < 30$ GeV, dominated by multijet events) to fill the missing events between the Monte Carlo prediction and observed data, see Fig. 4 (left). The overall normalization is determined in the W peak region (60 GeV $< m_T <$ 140 GeV).

A good agreement between data and Monte Carlo prediction is observed, see Fig. 4 (left and middle). In the data 630 events are reconstructed with $m_T >$ 150 GeV, compared to a background expectation of 623 ± 81 events. Two kinds of systematic uncertainties contribute in this analysis: global normalization uncertainties (cross sections, normalization, efficiency correction, multijet estimation) and shape changing uncertainties (electron energy scale and resolution, PDF uncertainty, uncertainty of the width of the W, jet energy scale). The overall systematic uncertainty on the background samples is of the order of 15%; the uncertainty on the signal samples varies between 15% and 50%.

A Bayesian approach [5] with flat prior leads to upper limits on the production cross section times branching fraction, $\sigma(p\bar{p} \to W' + X) \times B(W' \to e\nu)$. The limits, shown in Fig. 4 (right) as a function of the mass $m_{W'}$, are derived using a binned likelihood for the whole transverse mass spectrum $m_T > 150$ GeV. Comparing the observed limit with the theoretical prediction additional heavy charged gauge bosons can be excluded at the 95% CL up to 965 GeV, hence significantly improving upon the previous best limit of 800 GeV (DØ Run I [10]).

5 Summary

Final states with high energy objects are sensitive to a broad array of new physics. Three recent analyses have been presented which investigate the dielectron, diphoton, electron plus photon, and electron plus missing transverse energy final states using 1 fb^{-1} of data taken with the DØ experiment at the Tevatron proton-antiproton collider. Since no significant excess is observed in the data, new restrictive limits are set in all three cases.

References

1. Details for all DØ results can be found at http://www-d0.fnal.gov/Run2Physics/WWW/results.htm.
2. V. M. Abazov *et al.* (D0 Collaboration), Nucl. Instrum. Methods A **565**, 463 (2006).
3. L. Randall and R. Sundrum, Phys. Rev. Lett. **83**, 3370 (1999); ibid. **83**, 4690 (1999).
4. T. Sjöstrand *et al.*, Comput. Phys. Commun. **135**, 238 (2001).
5. I. Bertram *et al.*, FERMILAB-TM-2104 (2000).
6. H. Terazawa *et al.*, Phys. Lett. B **112**, 387 (1982); F. M. Renard, Il Nuovo Cimento **77 A**, 1 (1983); A. De Rujula, L. Maiani and R. Petronzio, Phys. Lett. B **140**, 253 (1984); E. J. Eichten, K. D. Lane and M. E. Peskin, Phys. Rev. Lett. **50**, 811 (1983); M. A. Shupe, Phys. Lett. B **86**, 87 (1979).
7. D. Acosta *et al.* (CDF Collaboration), Phys. Rev. Lett. **94**, 101802 (2005).
8. R. N. Mohapatra, Unification and Supersymmetry, Springer (2003).
9. G. Altarelli *et al.*, Z. Phys. C **45**, 109 (1989).
10. V. M. Abazov *et al.* (D0 Collaboration), Phys. Rev. D **69**, 111101 (2004).